

Synthesis of transactinide nuclei using radioactive beams

W. Loveland

Dept. of Chemistry, Oregon State University, Corvallis, Oregon 97331, USA

(Received 19 March 2007; published 24 July 2007)

The prospects for the synthesis of transactinide nuclei using radioactive beams are evaluated quantitatively for a modern radioactive beam facility. A simple formalism for calculating the complete fusion cross sections that reproduces the known heavy element production cross sections over six orders of magnitude is used to calculate the production rates for transactinide nuclei with $Z \leq 120$. All possible projectile and target combinations are evaluated. Exciting new possibilities for studies of the atomic physics, chemistry, and nuclear spectroscopy of the heaviest elements should be realized at a modern radioactive beam facility. The synthesis of new heavy elements is best undertaken at stable beam accelerators.

DOI: [10.1103/PhysRevC.76.014612](https://doi.org/10.1103/PhysRevC.76.014612)

PACS number(s): 25.70.Jj, 25.85.-w, 25.60.Pj

I. INTRODUCTION

One of the projected important uses [1] of new, modern radioactive beam facilities such as the proposed rare isotope accelerator (RIA) project [2,3] is the synthesis and study of the heaviest elements. Many interesting possibilities have been suggested [1], but quantitative estimates of what can actually be done are generally lacking. In this paper, the possibilities of synthesizing transactinide nuclei with radioactive beams at such a facility are evaluated quantitatively.

In Fig. 1, we show the predicted half-lives of the even-even transactinide nuclei. One observes an overall increase in half-life with increasing neutron number up to $N = 184$. This increase is thought to involve several orders of magnitude in half-life that could quantitatively change the character of studies of the atomic physics and chemistry of these elements. Thus attention has been focused on making new n -rich isotopes of the heaviest elements as well as the synthesis of new elements. Neutron-rich radioactive beams are thought to be suitable for this purpose.

Enhanced fusion cross sections have been observed for the reactions of neutron-rich ^{38}S with ^{181}Ta [6], ^{208}Pb [7], and $^{29,31}\text{Al}$ with ^{197}Au [8]. Liang *et al.* [9] have observed a fusion enhancement in the reaction of neutron-rich ^{132}Sn with ^{64}Ni . The enhanced fusion cross sections are due to a lowering of the fusion barrier for the neutron-rich projectiles. Stelson [10] has suggested that neutron flow effects with very n -rich projectiles could enhance fusion cross sections beyond a simple fusion barrier shift. Similar neutron flow phenomena have been described by Wang *et al.* [11,12]. Subbarrier fusion enhancements due to neutron transfer have also been suggested by Zagrebaev [13] and Kondratyev *et al.* [14]. In addition to enhanced fusion cross sections, one also expects increased survival probabilities for any heavy nuclei formed in these reactions because of the reduced fissility of the species and the lower excitation energies (due to the lowered fusion barriers).

Several authors have made specific suggestions regarding the use of radioactive beams to make new heavy nuclei. One of the early documents about the RIA project [15] stated that “Using beams of ^{8-11}Li , $^{10,11}\text{Be}$, $^{14-16}\text{C}$, $^{16-18}\text{N}$, $^{19-22}\text{O}$, $^{20-23}\text{F}$, $^{23-25}\text{Ne}$, and $^{24-31}\text{Na}$ with neutron-rich actinide

targets such as ^{244}Pu , ^{248}Cm , ^{249}Bk , $^{251,252}\text{Cf}$, and ^{254}Es , it will be possible to produce, identify and study the nuclear decay properties of a large number of neutron-rich actinide and transactinide isotopes.” Münzenberg [16] pointed out the need to have intense radioactive beams, *in excess of* $10^{14}/\text{s}$, to reach the region beyond $Z = 114$ with reasonable reaction rates, assuming current cross section systematics. Armbruster [17] estimates an evaporation residue (EVR) production cross section for the $^{208}\text{Pb}(^{80}\text{Ge},n)^{287}114$ reaction of 100 fb. Adamian *et al.* [18], using the dinuclear system (DNS) approach, estimate cross sections for cold fusion reactions involving a number of radioactive beams, ranging from ^{78}Ni to ^{92}Kr . Most of the cross sections are less than 1 pb, although the $^{208}\text{Pb}(^{78}\text{Ni},2n)^{284}\text{Ds}$ reaction cross section is estimated to be 36 pb. The expected increases in survival probability are negated by predicted decreases in P_{CN} , the probability that the dinuclear system formed at projectile-target contact will evolve inside the fission saddle point. Adamian *et al.* [19], using the DNS approach, examined the possibilities of using radioactive beams of ^{46}Ar , ^{47}K , and ^{50}Ca in hot fusion reactions to synthesize new heavy nuclei. The predicted complete fusion cross sections were similar to those found for stable ^{48}Ca . Zagrebaev [20] suggested the possible use of weakly bound neutron-rich projectiles, such as ^{26}F , ^{30}Na , ^{34}Mg , and ^{37}Si , in making n -rich transactinide nuclei, noting the need for projectile intensities greater than $10^8/\text{s}$ for these nuclei. The recent RISAC report [3] states that “where the intensity of the rare isotope is large ($^{90,92}\text{Kr}$, $^{90,92}\text{Sr}$, $\geq 10^{11}$ ions/s), fusion reactions become feasible with reaccelerated beams of high intensity and precise energies.” Aritomo [21] has suggested the possibility of synthesizing the doubly magic superheavy nucleus $^{298}114$ using hot fusion radioactive beam induced reactions such as $^{46}\text{Si} + ^{258}\text{Fm}$, $^{60}\text{Ca} + ^{244}\text{Pu}$, $^{72}\text{Cr} + ^{232}\text{Th}$, and $^{152}\text{La} + ^{152}\text{La}$. Aritomo calculates large cross sections for these reactions, ranging up to 10^6 pb, due to the high survival probabilities of the nuclei near $N = 184$.

In Sec. II of this paper, we discuss the calculational framework used to estimate the production rates of heavy nuclei with radioactive beams; while in Sec. III, we discuss tests of the calculational methods. In Sec. IV, we discuss the calculational results and their meaning. In Sec. V, we present the conclusions of this work.

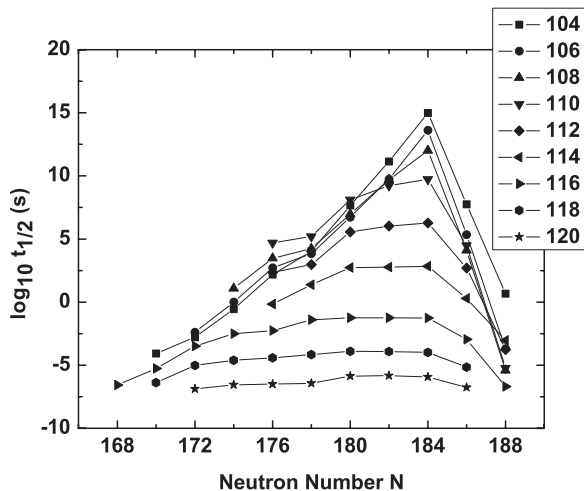


FIG. 1. Estimated total half-lives (considering α , β , and spontaneous fission decay) for the even-even transactinide nuclei with $Z = 104$ – 120 . The data are from Refs. [4,5].

II. CALCULATIONAL METHODS

We performed a brute force calculation to examine the possibilities of synthesizing new transactinide nuclei using radioactive beams. We started with the beam list of a typical, proposed modern radioactive beam facility, such as the now defunct rare isotope accelerator (RIA) [2]. We took the RIA beam list [22], which gives the identity and intensity of all the expected radioactive beams having suitable energies (less than 15A MeV), and considered all possible combinations of these projectile nuclei with all stable target nuclei (target thickness 1.0 mg/cm²) and all long-lived actinide nuclei (target thickness 0.5 mg/cm²). The beam intensities given in Ref. [22] were multiplied by 4 to simulate the effect of a 400 kW driver beam instead of the 100 kW assumed in Ref. [22]. A correction to the beam intensities given in Ref. [22] for radioactive decay of short-lived species [23] was made. For cold fusion reactions, the optimum excitation energy of the completely fused system was chosen to be 13 MeV. For hot fusion reactions, the optimum projectile energy was chosen by varying the excitation energy of the completely fused system from 30 to 60 MeV in 2 MeV steps. The yield of each product nucleus in atoms/day was calculated. No correction was made for the efficiency of any experimental apparatus that might be used to study these nuclei.

The conditions chosen for the calculations represent optimistic estimates for the input parameters. For example, in the reported synthesis of element 116 by the Dubna-Livermore Collaboration [24], the beam intensity was 1.2 pμA, target thickness was 0.34 mg/cm², separator efficiency was 35%, and focal plane detector efficiency was 87%, leading to an observed reaction rate of 0.6 atoms/day for a production cross section of 3.7 pb. (The production rate, using our calculational assumptions, would have been 2.5 atoms/day). Thus, under real experimental conditions, the observed time-averaged detection rates may be substantially less than the calculated production rates.

One might question the use of the RIA beam list [22] in these calculations because this project [2] in its original form is not likely to be built. However, recent plans [25] for modified versions of the RIA concept (“RIA-lite”) have indicated that the reaccelerated beam intensities will, in general, be similar to those given in the RIA beam list [22]. In any case, the RIA beam list serves as a benchmark against which future radioactive beam facility intensities can be compared. It is a relatively trivial task to scale the results described in this paper to intensities achieved in future accelerators.

The beam intensities for the more than 2300 beams given in Ref. [22] offer an important insight into the results obtained in the calculations. In Fig. 2, we show the projected intensities for the isotopes of the rare gases (Ne, Ar, Kr, and Xe) and some representative projectile nuclei (C, N, O, F, Na, Mg, Si, K, Ca, Ni, Ge, and Se). A horizontal line on each plot indicates the typical stable beam intensity (~ 1 pμA) used in heavy element syntheses, and the vertical line indicates the mass number of the most neutron-rich stable isotope of that element.

One immediately notes that very exotic beams (with 5–10 more neutrons than the most n -rich stable isotope) are produced with very low intensities, rendering them useless for heavy element synthetic reactions. For example, the nuclei ²⁶F, ³⁰Na, ³⁴Mg, or ³⁷Si are not available in the desired intensities [20] nor are the n -rich isotopes of Ni, Ge, Se, or Kr available at intensities commensurate with the predicted fb-pb cross sections [18]. Similarly, the intensities of ⁴⁶Si, ⁶⁰Ca, ⁷²Cr, and ¹⁵²La given in Ref. [22] are so low as to make the production rates for the reactions discussed by Aritomo [21] negligibly small. In fact, few radioactive beams are projected to have intensities of the magnitude of the stable beam intensities ($\sim 6 \times 10^{12}$ /s) used in heavy element synthesis reactions.

The cross section for the production of an evaporation residue, σ_{EVR} , can be written as

$$\sigma_{\text{EVR}} = \sigma_{\text{CN}} W_{\text{sur}}, \quad (1)$$

where σ_{CN} is the complete fusion cross section and W_{sur} is the survival probability of the completely fused system. The complete fusion cross section can be written as

$$\sigma_{\text{CN}} = \sum_{J=0}^{J_{\text{max}}} \sigma_{\text{capture}}(E_{\text{c.m.}}, J) P_{\text{CN}}(E_{\text{c.m.}}, J), \quad (2)$$

where $\sigma_{\text{capture}}(E_{\text{c.m.}}, J)$ is the capture cross section at center-of-mass energy $E_{\text{c.m.}}$ and spin J , and P_{CN} is the probability that the projectile-target system will evolve inside the fission saddle point to form a completely fused system rather than reseparating (quasifission).

Siwek-Wilczynska and Wilczynski [27], Siwek-Wilczynska *et al.* [28], and Swiatecki *et al.* [29] have developed a semiempirical formalism for predicting the capture cross sections for collisions leading to heavy nuclei. In the parametrization of Ref. [29], the capture cross section is given as

$$\sigma_{\text{capture}} = \pi R^2 \frac{v}{2E_{\text{c.m.}}} \left[X(1 + \text{erf } X) + \frac{1}{\sqrt{\pi}} \exp(-X^2) \right], \quad (3)$$

where

$$X = (E_{\text{c.m.}} - B)/v, \quad (4)$$

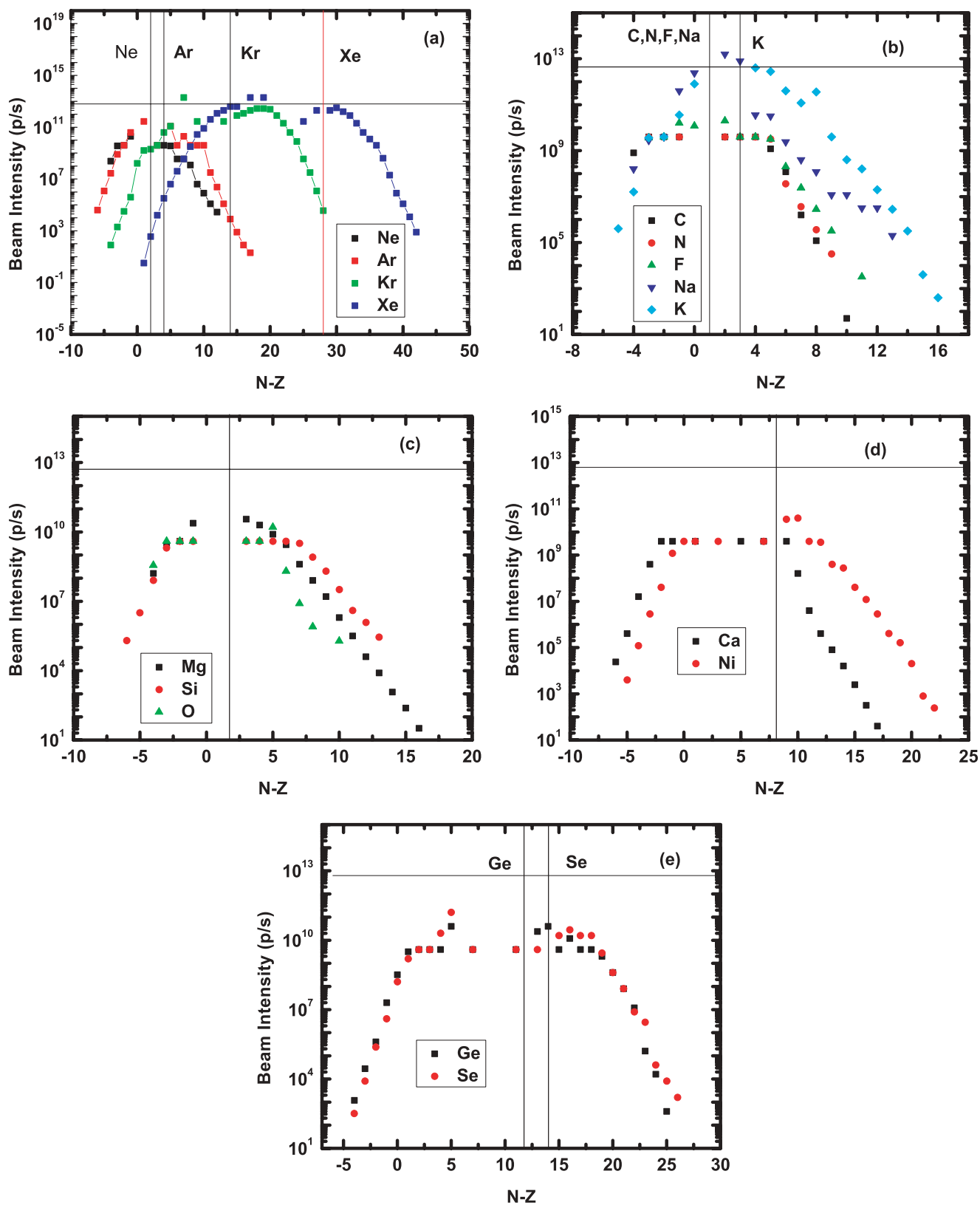


FIG. 2. (Color online) Estimated yields of representative reaccelerated beams from the proposed RIA project [22].

where

$$B = 0.85247z + 0.001361z^2 - 0.00000223z^3 \text{ MeV}, \quad (5)$$

where

$$z = \frac{Z_1 Z_2}{A_1^{1/3} + A_2^{1/3}}, \quad (6)$$

where Z_1 , A_1 , Z_2 , and A_2 are the atomic and mass numbers of the projectile and target nuclei, respectively. Also, in Eq. (4),

$$v = CB\sqrt{W_1^2 + W_2^2 + W_0^2}, \quad (7)$$

where

$$W_i^2 = \frac{R_i^2 \beta_i^2}{4\pi}, \quad (8)$$

where

$$R_i = 1.14A_i^{1/3} \text{ fm}, \quad (9)$$

and β_i = “ β_2 ” in Ref. [30], $C = 0.07767 \text{ fm}^{-1}$, $R = R_1 + R_2$, and $W_0 = 0.41 \text{ fm}$.

We note parenthetically that the results from this elaborate representation of σ_{capture} were compared with the simple formula [31] for the capture cross section at the barrier with reduced wavelength λ and orbital angular momentum ℓ

$$\sigma_{\text{capture}}^{\text{simple}} = \pi \lambda^2 \ell^2, \quad (10)$$

where ℓ^2 was $\sim 15^2$ with the result that $\sigma_{\text{capture}}^{\text{simple}}/\sigma_{\text{capture}}^{\text{semiempirical}} = 0.70 \pm 0.10$ for a group of reactions to make nuclei with $Z = 90$ –118. The values of σ_{capture} are typically 10–100 mb.

The survival probability W_{sur} can be written as

$$W_{\text{sur}} = P_{xn}(E_{\text{CN}}^*) \prod_{i=1}^{i_{\text{max}}=x} \left(\frac{\Gamma_n}{\Gamma_n + \Gamma_f} \right)_{i,E^*}, \quad (11)$$

where the index i is equal to the number of emitted neutrons, and P_{xn} is the probability of emitting exactly x neutrons [32]. In evaluating the excitation energy in Eq. (4), we start at the excitation energy E^* of the completely fused system and reduce it for each evaporation step by the binding energy of the emitted neutron and an assumed neutron kinetic energy of $2T$, where $T = (E^*/a)^{1/2}$ is the temperature of the emitting system. For calculating Γ_n/Γ_f , we used the classical formalism from Vandenbosch and Huizenga [33]

$$\frac{\Gamma_n}{\Gamma_f} = \frac{4A^{2/3}(E^* - B_n)}{k[2a^{1/2}(E^* - B_f)^{1/2} - 1]} \exp[2a^{1/2}(E^* - B_n)^{1/2} - 2a^{1/2}(E^* - B_f)^{1/2}], \quad (12)$$

where A is the mass number of the emitting/fissioning system. The constants k and a are taken to be 9.8 MeV and $(A/12) \text{ MeV}^{-1}$, respectively. The fission barriers B_f are written as the sum of liquid drop, B_f^{LD} , and shell correction terms as

$$B_f(E^*) = B_f^{\text{LD}} + U_{\text{shell}} \exp[-\gamma E^*], \quad (13)$$

where

$$\gamma^{-1} = 5.48A^{1/3}/(1 + 1.3A^{-1/3}) \text{ MeV}, \quad (14)$$

and the shell correction energies U_{shell} to the LDM barriers are taken from Ref. [30], the liquid drop barriers are taken from Ref. [34], and the fade-outs of the shell corrections with increasing excitation energy are taken from Ignatyuk *et al.* [35]. Neutron binding energies B_n are taken from Ref. [30]. Collective enhancement effects are only important for spherical product nuclei, and they are calculated using the semiempirical formalism of Ref. [17], where the collective enhancement factor multiplies $\frac{\Gamma_n}{\Gamma_f}$ and is written as $K_{\text{vib}}/K_{\text{rot}}f(E^*/E_{\text{crit}})$, where $K_{\text{rot}} = 1.4 \times 10^{-2}A^{5/3}T(1 + \beta_2/3)$, where β_2 is the deformation parameter, and $K_{\text{vib}} = (1 + 0.14\Delta N + 0.23\Delta Z)^2$, where ΔN and ΔZ are the numbers of valence nucleons or valence holes with respect to the next doubly closed shell nucleus with $f(E^*/E_{\text{crit}}) = [1 + \exp((E^* - E_{\text{crit}})/d_{\text{crit}})]^{-1}$, where $E_{\text{crit}} = 40 \text{ MeV}$ and $d_{\text{crit}} = 10 \text{ MeV}$. We used a semiempirical form for P_{CN}

$$P_{\text{CN}}(E, J) \approx P_{\text{CN}}(E) = 0.5 \exp[-c(x_{\text{eff}} - x_{\text{thr}})], \quad (15)$$

where the effective fissility, x_{eff} , is defined as

$$x_{\text{eff}} = \left[\frac{(Z^2/A)}{(Z^2/A)_{\text{crit}}} \right] (1 - \alpha + \alpha f(\kappa)), \quad (16)$$

where

$$(Z^2/A)_{\text{crit}} = 50.883 \left[1 - 1.7826 \left(\frac{(N - Z)}{A} \right)^2 \right], \quad (17)$$

with Z , N , and A the atomic number, neutron number, and mass number of the completely fused system, and where

$$f(\kappa) = \frac{4}{\kappa^2 + \kappa + \frac{1}{\kappa} + \frac{1}{\kappa^2}}. \quad (18)$$

The parameter $\alpha = 1/3$, and the parameter $\kappa = (A_1/A_2)^{1/3}$, where A_1 and A_2 are the mass numbers of the projectile and target nuclei, respectively. This form for P_{CN} is similar to the one used by Armbruster [17] to define $p(B_B)$, the fusion probability at the Bass barrier (B_B) for central collisions [26]. We used this form and fitted the known data [36] in 63 well-characterized hot and cold fusion reactions to synthesize heavy nuclei with $Z = 102$ –118 to determine the values of the coefficients c and x_{thr} for cold and hot fusion reactions. The best fit to the cold fusion data gave $c = 136.5$ and $x_{\text{thr}} = 0.79$. For the hot fusion reactions, the best fit for $x_{\text{eff}} \leq 0.80$ was $c = 104$ and $x_{\text{thr}} = 0.69$; while for $x_{\text{eff}} \geq 0.80$, $c = 82$ and $x_{\text{thr}} = 0.69$.

III. TESTS OF THE CALCULATIONAL MODEL

The results of using this simple calculational model to predict the cross sections for the synthesis of heavy nuclei are shown in Figs. 3 and 4. In Fig. 3, we show the calculated and measured [36] cross sections for the synthesis of elements 102–113 using cold fusion reactions. The agreement between the measured and calculated cross sections is satisfactory, as the average ratio of measured to calculated values is 1.6 ± 3.5 , with 95% confidence limits of 0.1–36. In Fig. 4, we show the same information for hot fusion reactions; the data are for 43 well-known reactions [36] of lighter

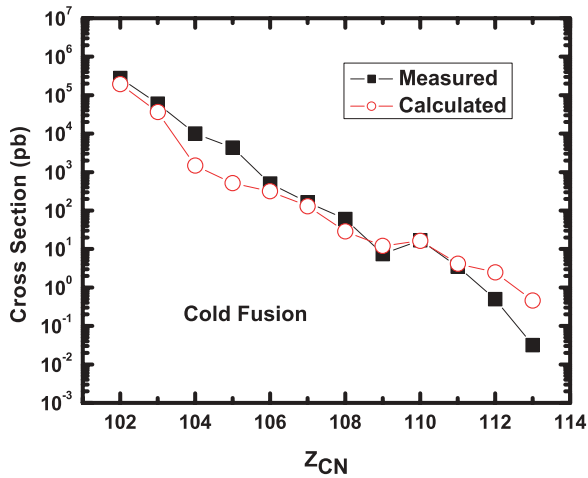


FIG. 3. (Color online) Calculated and measured values of the evaporation residue production cross sections for the synthesis of elements 102–113 using cold fusion reactions.

ions with actinide targets that produce completely fused systems with $102 \leq Z \leq 118$, including recent results from the Dubna-Livermore Collaboration for the synthesis of elements 112–118. The agreement between calculated and measured cross sections is not as good as for cold fusion reactions, presumably because of the difficulty posed by calculation of the survival probabilities in systems where three to six neutrons are being evaporated, with the resulting compounding of errors. The average value of the ratio of measured to calculated cross sections is 1.4 ± 7.3 with 95% confidence level limits of 0.06–70. To pursue this point further, we show in Fig. 5 the calculated and measured values of the survival probabilities for a series of 32 reactions [37] involving lighter projectiles and actinide target nuclei that produce compound nuclei with an effective fissility, $x_{\text{eff}} \leq 0.68$. For these reactions, we assume $P_{\text{CN}} = 1$ and that the survival probabilities can be calculated directly from the ratio of the measured evaporation residue production cross sections and

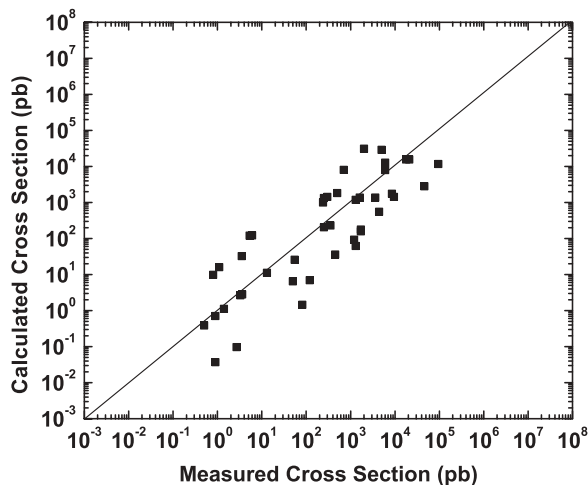


FIG. 4. Calculated and measured values of the evaporation residue production cross sections for the synthesis of 43 well-characterized nuclei with $102 \geq Z \geq 118$ using hot fusion reactions.

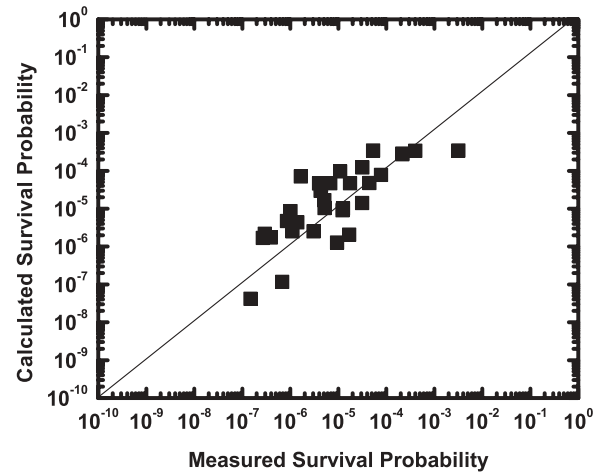


FIG. 5. Calculated and measured values of the survival probabilities for a series of hot fusion reactions.

the capture cross sections predicted in Ref. [29]. The average value of the ratio of measured to calculated values is 0.5 ± 4.5 with 95% confidence limits of 0.1–40, indicating the difficulty of predicting this quantity accurately in reactions in which three to six neutrons are being evaporated, even when the neutron binding energies and fission barriers are relatively well known. (If we neglect the energy variation of Γ_n/Γ_f and P_{xn} , and use the average number of evaporated neutrons in these reactions as being five, then the ratio of the observed to calculated value of the survival probability for each step in the chain is 0.87, a relatively good agreement between measured and calculated values). In short, with 95% confidence, we can say that the cross sections calculated by this simple model for cold fusion reactions are roughly correct within a factor of 10 with a tendency to underestimate the cross sections. For hot fusion reactions, at the 95% confidence level, we can say that the cross sections calculated by this simple model are correct within a factor of 20, with a tendency to underestimate the cross sections.

One may wonder if a more sophisticated model for calculating the cross sections should have been employed. In our brute force approach, we evaluated over 150 000 candidate reactions involving stable beams and 1.6 million candidate reactions involving radioactive beams. The final calculations involved 320 cold fusion reactions involving stable beams and 2075 cold fusion reactions involving radioactive beams, leading to the production of $Z = 102$ –120 nuclei with rates ≥ 0.001 atoms/day. The final calculations also involved 141,472 hot fusion reactions involving stable beams and 1,581,008 hot fusion reactions involving radioactive beams, leading to $Z = 102$ –120 nuclei with production rates ≥ 0.001 atoms/day. Additional calculations were needed to calibrate and test the formalism. These estimates do not involve cases in which the calculated production rates were ≤ 0.001 atoms/day, and thus they represent lower limits on the total number of calculations performed. A simple, easily evaluated model was essential for making these voluminous calculations.

In Fig. 6, we compare the values of P_{CN} deduced in this work for cold fusion reactions with other estimates of this

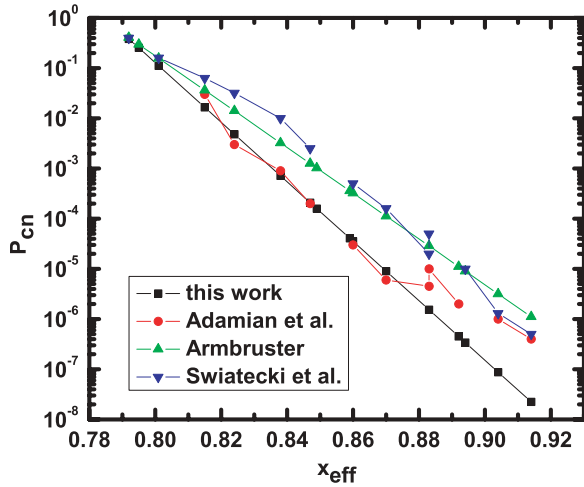


FIG. 6. (Color online) Calculated values of P_{CN} for a series of cold fusion reactions.

variable [18,29,31]. There is reasonable agreement between the our deduced values of P_{CN} and those calculated by Adamian *et al.* [18], using the dinuclear system (DNS) model; although there are discrepancies for the highest Z products, where the influence of the $Z = 114$ shell on W_{sur} in our calculations causes a further suppression of P_{CN} . For the cold fusion syntheses of elements 108 and 109 ($x_{eff} = 0.86-0.87$), the disagreement in P_{CN} values exceeds the expected uncertainty in W_{sur} values for these $1n$ reactions.

IV. RESULTS AND DISCUSSION

In Fig. 7(a), we show the maximum predicted production rates for cold fusion reactions for isotopes of elements 102–120, using stable and radioactive beams. (Stable beam intensities were assumed to be $1 \mu A$.) For most elements, stable beam production is predicted to be the most favorable method of production, although production using radioactive beams becomes comparable to stable beam production for $Z \geq 118$ [Fig. 7(b)]. The details behind these plots are summarized in Table I. (Please note that, as remarked earlier, real detection rates will be substantially less than the predicted production rates. Production rates of ≤ 0.1 atoms/day indicate situations that are not good candidates for study with today’s technology). While the choices of the best stable beam reactions are “conventional,” mirroring past successes, the choice of the best radioactive beam reactions bears further comment. It is clearly the “cross section \times beam intensity” factor that governs the choice of reactions, resulting in the choice of projectiles near stability because of their expected higher intensity. It is only for special volatile species, such as the rare gases and alkali metals, that one sees deviations from this idea.

In Fig. 8, we show the ratio of the best hot fusion rates for hot fusion production of isotopes of elements 102–120 using stable and radioactive beams. Table II contains the details behind Fig. 8. The caveat issued earlier regarding the calculated production rates is especially important here. Some of the reactions with highest yields involve hard to handle or

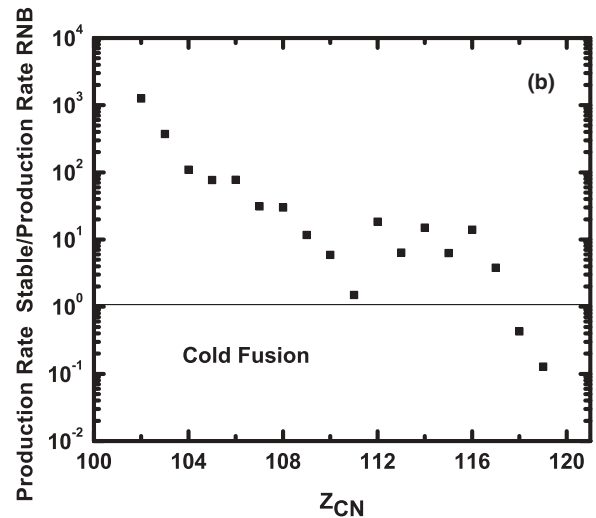
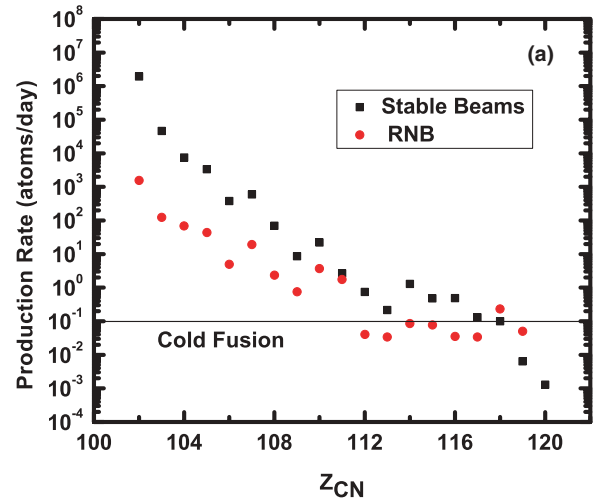


FIG. 7. (Color online) Comparison of production rates using cold fusion reactions.

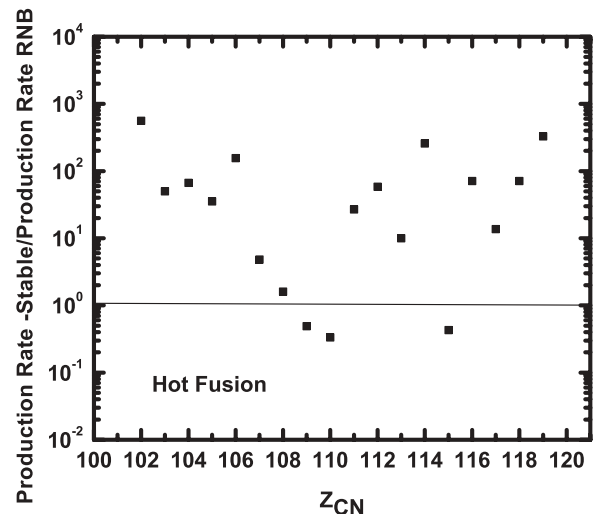


FIG. 8. Comparison of production rates using hot fusion reactions.

TABLE I. Comparison of best stable beam and radioactive beam cold fusion production reactions for $Z = 102 - 120$.

Z	Best stable reaction	σ (pb)	ϕ	Best RNB reaction	σ (pb)	ϕ
102	$^{208}\text{Pb}(^{48}\text{Ca},n)$	190 000	6.2×10^{12}	$^{208}\text{Pb}(^{49}\text{Ca},n)$	1 240 000	4×10^9
103	$^{209}\text{Bi}(^{48}\text{Ca},n)$	36 400	6.2×10^{12}	$^{208}\text{Pb}(^{49}\text{Ca},n)$	150 000	4×10^9
104	$^{208}\text{Pb}(^{50}\text{Ti},n)$	1 460	6.2×10^{12}	$^{208}\text{Pb}(^{51}\text{Ti},n)$	5 190	4×10^9
105	$^{209}\text{Bi}(^{50}\text{Ti},n)$	514	6.2×10^{12}	$^{208}\text{Pb}(^{54}\text{V},n)$	11 700	3.6×10^9
106	$^{208}\text{Pb}(^{54}\text{Cr},n)$	316	6.2×10^{12}	$^{208}\text{Pb}(^{57}\text{Cr},n)$	8 890	2.8×10^9
107	$^{209}\text{Bi}(^{54}\text{Cr},n)$	130	6.2×10^{12}	$^{208}\text{Pb}(^{58}\text{Mn},n)$	3 210	8×10^9
108	$^{208}\text{Pb}(^{57}\text{Fe},n)$	29	6.2×10^{12}	$^{208}\text{Pb}(^{61}\text{Fe},n)$	3 380	4×10^9
109	$^{209}\text{Bi}(^{57}\text{Fe},n)$	12	6.2×10^{12}	$^{208}\text{Pb}(^{58}\text{Co},n)$	2.4	4×10^{12}
110	$^{208}\text{Pb}(^{64}\text{Ni},n)$	16	6.2×10^{12}	$^{208}\text{Pb}(^{65}\text{Ni},n)$	497	3.6×10^{10}
111	$^{209}\text{Bi}(^{64}\text{Ni},n)$	4.2	6.2×10^{12}	$^{208}\text{Pb}(^{66}\text{Cu},n)$	60	2.8×10^{11}
112	$^{208}\text{Pb}(^{70}\text{Zn},n)$	2.4	6.2×10^{12}	$^{209}\text{Bi}(^{66}\text{Cu},n)$	5.7	2.8×10^{11}
113	$^{209}\text{Bi}(^{70}\text{Zn},n)$	0.5	6.2×10^{12}	$^{208}\text{Pb}(^{74}\text{Ga},n)$	18.9	1.2×10^{11}
114	$^{208}\text{Pb}(^{76}\text{Ge},n)$	1.5	6.2×10^{12}	$^{209}\text{Bi}(^{80}\text{Ga},n)$	34.5	2×10^9
115	$^{209}\text{Bi}(^{76}\text{Ge},n)$	0.6	6.2×10^{12}	$^{208}\text{Pb}(^{78}\text{As},n)$	7.6	8×10^{10}
116	$^{208}\text{Pb}(^{82}\text{Se},n)$	0.6	6.2×10^{12}	$^{208}\text{Pb}(^{85}\text{Se},n)$	17.6	1.6×10^{10}
117	$^{209}\text{Bi}(^{82}\text{Se},n)$	0.2	6.2×10^{12}	$^{208}\text{Pb}(^{89}\text{Br},n)$	3.4	8×10^{10}
118	$^{208}\text{Pb}(^{86}\text{Kr},n)$	0.02	6.2×10^{12}	$^{208}\text{Pb}(^{91}\text{Kr},n)$	0.7	2.8×10^{12}
119	$^{209}\text{Bi}(^{86}\text{Kr},n)$	0.008	6.2×10^{12}	$^{208}\text{Pb}(^{90}\text{Rb},n)$	0.1	3.6×10^{12}
120	$^{208}\text{Pb}(^{87}\text{Sr},n)$	0.002	6.2×10^{12}			

exotic targets such as ^{252}Cf and ^{253}Es , and many of the best radioactive beam reactions involve the use of a ^{24}Na projectile, as ^{24}Na is one of the nuclides on the RIA beam list [22] whose intensity ($\sim 2.5 \text{ p}\mu\text{A}$) exceeds that of typical stable beams. In general, for hot fusion reactions, stable beams are preferred to radioactive beams for heavy element production, although there are regions ($Z = 108-110$ and $Z = 115$) where radioactive beams may offer advantages. The average value of the ratio of the production rates for stable to radioactive beams for the data of Figs. 7 and 8 is ~ 100 . [The large discrepancy between predicted and observed cross sections for the hot

fusion synthesis of elements 114 and 116 using stable beams (121 vs 5.3 pb, and 60 vs 3.3 pb) is due to the strong influence of the $Z = 114$ shell in Ref. [30] which affects the calculated fission barrier heights and survival probabilities.]

However, the point of using n -rich radioactive beams in the study of the heaviest elements is to form very neutron-rich isotopes of these elements, not reachable in reactions with stable nuclei. Accordingly, we show in Figs. 9–12 the nuclidic production rates for cold and hot fusion reactions using stable and radioactive beams. (Detailed plots for each Z from $Z = 102$ to $Z = 120$ are available [38].) In

TABLE II. Same as Table I, but for hot fusion production reactions.

Z	Best stable reaction	σ (pb)	ϕ	Best RNB reaction	σ (pb)	ϕ
102	$^{243}\text{Am}(^{14}\text{N},3n)$	2 900 000	6.2×10^{12}	$^{248}\text{Cm}(^{16}\text{C},4n)$	8 100 000	4×10^9
103	$^{248}\text{Cm}(^{14}\text{N},5n)$	2 200 000	6.2×10^{12}	$^{238}\text{U}(^{24}\text{Na},5n)$	16 200	1.6×10^{13}
104	$^{249}\text{Bk}(^{14}\text{N},5n)$	2 700 000	6.2×10^{12}	$^{237}\text{Np}(^{24}\text{Na},5n)$	1 550	1.6×10^{13}
105	$^{252}\text{Cf}(^{14}\text{N},3n)$	340 000	6.2×10^{12}	$^{244}\text{Pu}(^{24}\text{Na},5n)$	3 630	1.6×10^{13}
106	$^{249}\text{Bk}(^{19}\text{F},5n)$	715	6.2×10^{12}	$^{252}\text{Cf}(^{21}\text{O},5n)$	2 500 000	1.6×10^{10}
107	$^{253}\text{Es}(^{18}\text{O},4n)$	40 800	6.2×10^{12}	$^{248}\text{Cm}(^{24}\text{Na},5n)$	3 200	1.6×10^{13}
108	$^{252}\text{Cf}(^{22}\text{Ne},4n)$	4 940	6.2×10^{12}	$^{249}\text{Bk}(^{24}\text{Na},5n)$	1 220	1.6×10^{13}
109	$^{253}\text{Es}(^{22}\text{Ne},4n)$	3 030	6.2×10^{12}	$^{252}\text{Cf}(^{24}\text{Na},5n)$	2 000	1.6×10^{13}
110	$^{246}\text{Cm}(^{30}\text{Si},4n)$	224	6.2×10^{12}	$^{253}\text{Es}(^{24}\text{Na},5n)$	275	1.6×10^{13}
111	$^{249}\text{Bk}(^{30}\text{Si},4n)$	96	6.2×10^{12}	$^{238}\text{U}(^{42}\text{K},5n)$	5.2	4×10^{12}
112	$^{250}\text{Cf}(^{30}\text{Si},4n)$	17	6.2×10^{12}	$^{237}\text{Np}(^{43}\text{K},4n)$	0.6	2.8×10^{12}
113	$^{249}\text{Bk}(^{36}\text{S},4n)$	11	6.2×10^{12}	$^{244}\text{Pu}(^{42}\text{K},5n)$	1.7	4×10^{12}
114	$^{244}\text{Pu}(^{48}\text{Ca},4n)$	120	6.2×10^{12}	$^{248}\text{Cm}(^{46}\text{Ar},4n)$	740	4×10^9
115	$^{253}\text{Es}(^{36}\text{S},4n)$	2.3	6.2×10^{12}	$^{248}\text{Cm}(^{46}\text{K},5n)$	91	3.6×10^{11}
116	$^{248}\text{Cm}(^{48}\text{Ca},4n)$	60	6.2×10^{12}	$^{249}\text{Bk}(^{43}\text{K},4n)$	1.9	2.8×10^{12}
117	$^{249}\text{Bk}(^{48}\text{Ca},4n)$	17	6.2×10^{12}	$^{252}\text{Cf}(^{46}\text{K},5n)$	22	3.6×10^{11}
118	$^{252}\text{Cf}(^{48}\text{Ca},4n)$	7.8	6.2×10^{12}	$^{253}\text{Es}(^{46}\text{K},5n)$	2	3.6×10^{11}
119	$^{253}\text{Es}(^{48}\text{Ca},4n)$	1.6	6.2×10^{12}	$^{209}\text{Bi}(^{92}\text{Kr},4n)$	0.01	3.6×10^{11}
120	$^{252}\text{Cf}(^{50}\text{Ti},4n)$	0.03	6.2×10^{12}			

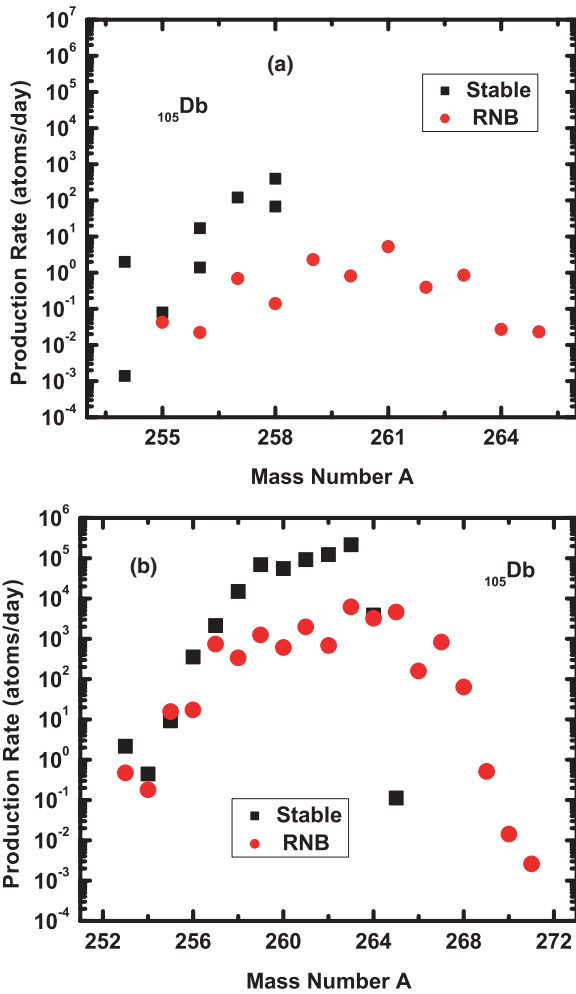


FIG. 9. (Color online) Comparison of production rates of Db isotopes with (a) cold fusion reactions and (b) hot fusion reactions.

Figs. 9–10, we show typical patterns for $Z = 102$ – 110 nuclei. For cold fusion reactions, the use of radioactive beams greatly increases the number of neutron-rich nuclei that can be produced, although the production rates are not high. For Db isotopes produced by cold fusion, the best stable beam reactions are conventional reactions such as $^{209}\text{Bi}(^{50}\text{Ti},n)$, $^{209}\text{Bi}(^{49}\text{Ti},n)$, etc. For radioactive beams, the best reactions involve $^{208}\text{Pb}(^{54-58}\text{V},n)$ reactions. Higher yields extending to more n -rich Db nuclei are expected for hot fusion reactions. Here the radioactive beam reactions form a “tail of yields” leading to very n -rich nuclei. (The heaviest known directly produced isotope of Db is ^{263}Db ; heavier isotopes are reported in the decay of elements 112 and 113.) The calculations suggest the direct production of the Db isotopes out to ^{268}Db at reasonable rates. Typical stable beam reactions are $^{249}\text{Cf}(^{14}\text{N},5n)$, and typical radioactive beam reactions are $^{244}\text{Pu}(^{24,25}\text{Na}, 4-5n)$. A qualitatively similar situation occurs for the production of Hs nuclei where the heaviest known isotope is ^{270}Hs . The production rates for very n -rich nuclei from cold or hot fusion reactions is not very encouraging. Stable beam reactions will likely take one as far as one can go with these nuclei.

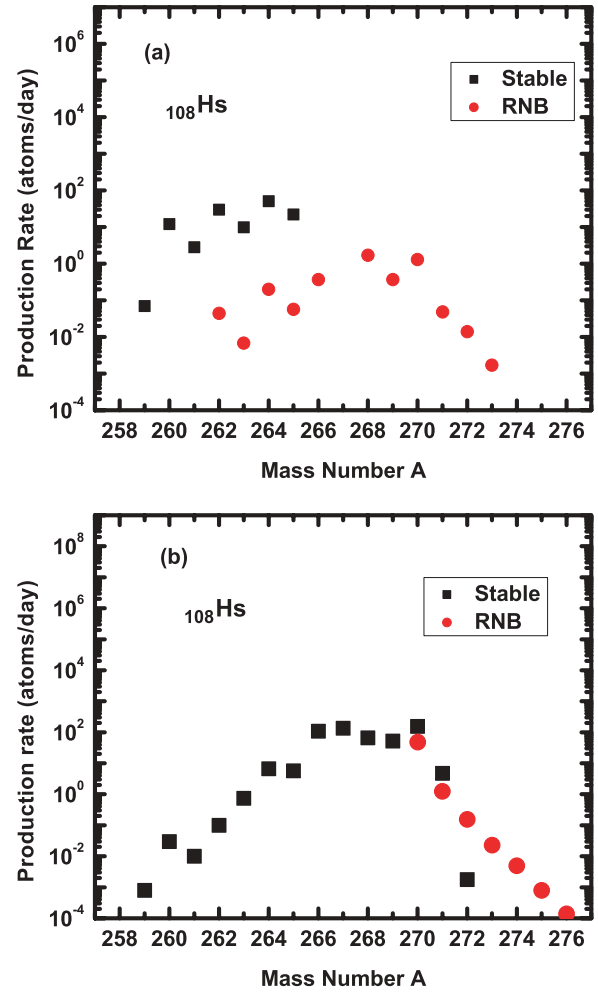


FIG. 10. (Color online) Same as Fig. 9, but for Hs isotopes.

In Figs. 11–12, we show some representative cases for the production of isotopes of elements 111–120. While radioactive beams can lead to more n -rich nuclei not produced with stable beams, the predicted yields (≤ 0.1 atoms/day) are so low as to be marginal. Because of the difficulty of producing these very heavy nuclei, stable beams are favored.

One of the promises of the use of radioactive beams in heavy element research is the production of long-lived neutron-rich nuclei for the studies of the atomic physics and chemistry of these elements. In Table III, we show for elements 102–109 the heaviest known directly produced isotope of that element and its half-life. We also show heavier isotopes of each element that are predicted to be formed using radioactive beams at levels of ≥ 1 atom/day and the predicted α -decay half-lives of each nuclide. The α -decay half-lives were estimated using the Sobczewski-Parkhomenko relationships [39] and Q_α values calculated from the 2003 mass evaluation of Audi, Wapstra, and Thibault [40]. In every case, except for Hs where the known ^{270}Hs is exactly at the $N = 162$ shell, an increase of one or more orders of magnitude in half-life is expected for the new neutron-rich nuclei produced by radioactive beams. In some cases, there are increases of three orders of magnitude leading to species with half-lives of hours to many months. Such

TABLE III. Long-lived neutron-rich nuclei produced by radioactive beam reactions with $Z = 103\text{--}109$.

Element	Heaviest known isotope produced directly	$t_{1/2}$	Predicted new isotopes and their predicted half-lives
Lr	262	216 min	(263, 12 h)(264, 80 d)(265, 196 d)
Rf	263	15 min	(264, 9.0 min)(265, 12.4 h)
Db	263	27 s	(264, 3.6 min)(265, 3.4 min)(266, 2.4 h)(267, 7.2 h) (268, 2.4 h)
Sg	266	21 s	(267, 4.2 min)(268, 7.1 min)(269, 1.3 min) (270, 2.6 s)
Bh	267	17 s	(268, 47 s)(269, 1.4 min)(270, 10.6 s)(271, 0.8 s)(272, 9.9 s)
Hs	270		(271, 0.13 s)(272, 0.02 s)(273, 0.13 s)(274, 0.83 s)
Mt	268	42 ms	(269, 6.4 ms)(270, 54 ms)(271, 69 ms)(272, 12 ms) (273, 1.2 ms)(274, 20.9 ms)(275, 78 ms)

changes should qualitatively affect the character of chemical and atomic physics studies of these elements.

The half-life variations of the n -rich nuclei shown in Table III also reveal the influence of the predicted $N = 162$ shell closure, which can be directly reached for each atomic number. (Some controversy exists regarding the nature of probable shell closures at $N = 162$ or $N = 164$ [41]). We

simply point out that the availability of additional n -rich nuclei in this region can help resolve these questions.

In Fig. 13, we show a global comparison of the production of heavy nuclei by either stable or radioactive beams. Specifically, we plot the \log_{10} of the ratio of the best stable beam production rate to the best radioactive beam production rate for each heavy nuclide from $Z = 102$ to $Z = 119$. We have chosen

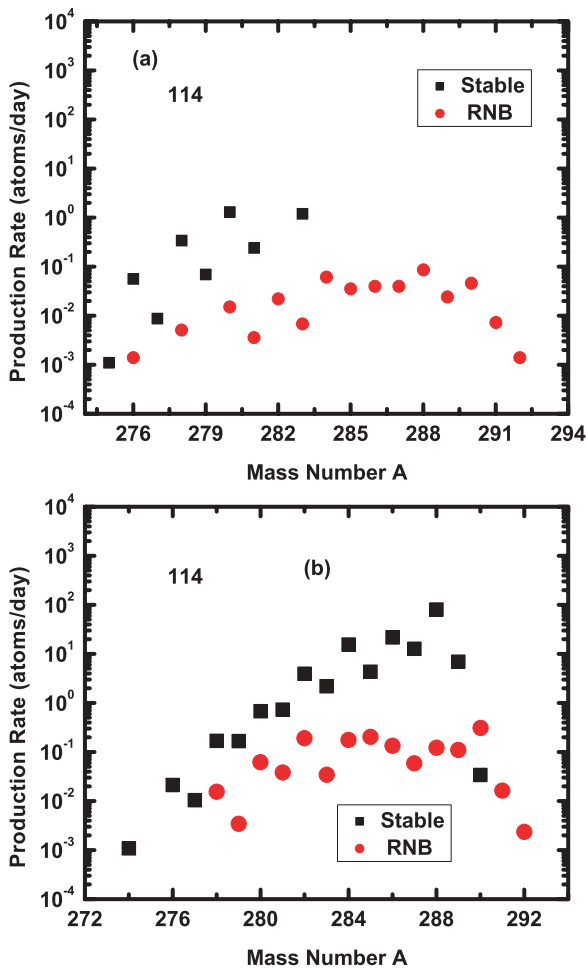


FIG. 11. (Color online) Comparison of production rates of 114 isotopes with (a) cold fusion reactions and (b) hot fusion reactions.

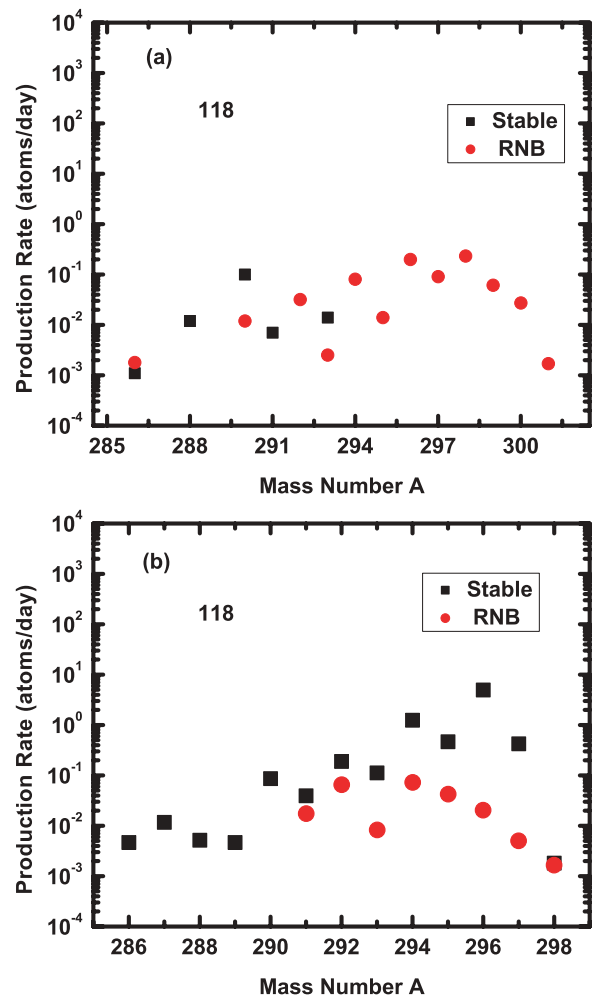


FIG. 12. (Color online) Same as Fig. 11, but for 118 isotopes.

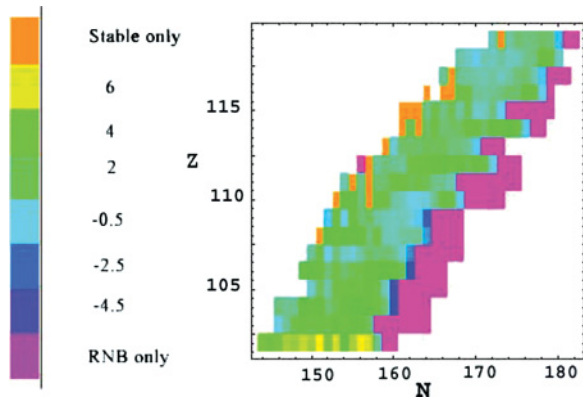


FIG. 13. (Color online) Contour plot of the \log_{10} value of the ratio of the production rate by stable beams to the production rate by radioactive beams vs the Z , N of each product nuclide.

the best production rates for each product irrespective of whether hot or cold fusion reactions were employed. Clearly, a number of neutron-rich nuclei can only be made using radioactive beams. As pointed out earlier, these nuclei should be important for studies of the atomic physics, chemistry, and nuclear spectroscopy of the heavy elements. For most nuclei that can be formed by either stable or radioactive beam induced reactions, the stable beam reactions give production rates that are about 100 times larger. There are a small number of n -deficient nuclei that can only be produced in practical quantities with stable beams.

What about the oft-repeated mantra that radioactive beams will greatly enhance our ability to study and understand the physics of the heaviest elements? As for the specific claims described in Refs. [15–21], they are, for the most part, unsustainable because they have not quantitatively evaluated a cross section \times beam intensity product. Some of the claims [15] that point to the use of lighter neutron-rich radioactive beams in heavy element research are quite true and point to the real promise of radioactive beams in heavy element research.

How can the simple estimates of this paper be improved? Clearly, the weakest point of most of the cross section estimates is the calculation of the survival probabilities of highly excited transactinide nuclei. Measurements that unfold the effect of multiple chance fission at higher excitation energies for high Z nuclei will help one to better physically constrain the calculations. Better estimates of the isospin dependence of the fusion hindrance for very n -rich nuclei would be helpful, especially in light of fragmentary evidence [42] of a lessening of this hindrance for n -rich nuclei. Our calculations include the effect of a lowered fusion barrier for n -rich projectiles, but they do not include any possible effects of fusion enhancement beyond a simple barrier shift. More sophisticated model calculations treating a smaller number of promising cases would be especially welcome. While one would never expect

a radioactive beam facility to be built just for heavy element research, to the extent that such research drives the construction of new facilities, the most promising paths seem to involve the use of lighter n -rich beams of very high intensity. Fission fragment projectiles are predicted to have significant fusion hindrance that detracts from their use in heavy element research. In another vein, until radioactive beam facilities produce beams of intensities comparable to those given in Ref. [22], their impact on heavy element research will not be great.

V. CONCLUSIONS

What have we learned from this calculational exercise? We conclude the following:

- (i) The use of radioactive beams in the synthesis of heavy nuclei can lead to the formation, at reasonable rates, of a group of neutron-rich nuclei not reachable with stable beams. These nuclei are predicted to have longer half-lives than existing nuclei and should be important for nuclear spectroscopy and studies of the atomic physics and chemistry of the heaviest elements.
- (ii) The best (i.e., highest production rate) reactions for producing these nuclei involve the use of lighter n -rich radioactive beams, i.e., containing a few neutrons more than the most stable n -rich isotope of that element, thought to be produced with higher intensities at modern radioactive beam facilities.
- (iii) When considering reactions involving radioactive beams, it is important to evaluate the cross section \times beam intensity product, as many postulated reactions involve beams of low intensity or reduced cross sections.
- (iv) The best way to produce most heavy nuclei, especially those of high Z , is to use stable beams.

ACKNOWLEDGMENTS

I gratefully acknowledge the help of several people in performing the calculations described in this work. Mike Cloughesy, a high school summer student, and Zach Evenson, a physics undergraduate student, contributed to the development of the calculational model used in this work. Helpful discussions with K. E. Gregorich were important in formulating the ideas used in the calculations. Most of the work was done while I was a guest of the nuclear chemistry group of Prof. H. Nitsche at the Lawrence Berkeley Laboratory, and I appreciate their moral and financial support during this period. Financial support was provided by the Office of High Energy and Nuclear Physics, Nuclear Physics Division, U.S. Dept. of Energy, under Grant No. DE-FG06-97ER41026.

[1] DOE/NSF Nuclear Science Advisory Committee, Opportunities in Nuclear Science, A Long Range Plan for the Next Decade, April 2002 (unpublished); Committee on Nuclear Physics,

National Research Council, *Nuclear Physics: The Core of Matter*, The Fuel of Stars (National Academies Press, Washington, 1999).

- [2] <http://www.phy.anl.gov/ria>
- [3] Rare Isotope Science Assessment Committee, National Research Council, *Scientific Opportunities with a Rare-Isotope Facility in the United States* (National Academies Press, Washington, 2007).
- [4] R. Smolańczuk, Phys. Rev. C **56**, 812 (1997).
- [5] P. Moller, J. R. Nix, and K. L. Kratz, At. Data Nucl. Data Tables **66**, 313 (1997).
- [6] K. E. Zyranski *et al.*, Phys. Rev. C, **63**, 024615 (2001).
- [7] W. Loveland, D. Peterson, A. M. Vinodkumar, P. H. Sprunger, D. Shapira, J. F. Liang, G. A. Souliotis, D. J. Morrissey, and P. Lofy, Phys. Rev. C **74**, 044607 (2006).
- [8] Y. X. Watanabe *et al.*, Eur. Phys. J. A **10**, 273 (2001).
- [9] J. F. Liang, Phys. Rev. Lett. **91**, 152701 (2003).
- [10] P. Stelson, Phys. Lett. **B205**, 190 (1988).
- [11] Ning Wang, Xizhen Wu, and Zhuxia Li, Phys. Rev. C **67**, 024604 (2003)
- [12] Ning Wang, Zhuxia Li, and Xizhen Wu, Phys. Rev. C **65**, 064608 (2002)
- [13] V. I. Zagrebaev, Phys. Rev. C **67**, 061601(R) (2003).
- [14] V. N. Kondratyev, A. Bonasera, and A. Iwamoto, Phys. Rev. C **61**, 044613 (2000)
- [15] IsoSpin Laboratory (ISL), LALP 91-51, 1991 (unpublished).
- [16] G. Müntzenberg, Philos. Trans. R. Soc. London Ser. A **356**, 2085 (1998).
- [17] P. Armbruster, Rep. Prog. Phys. **62**, 465 (1999).
- [18] G. G. Adamian, N. V. Antonenko, and W. Scheid, Nucl. Phys. **A678**, 24 (2000).
- [19] G. G. Adamian, N. V. Antonenko, and W. Scheid, Phys. Rev. C **69**, 044601 (2000).
- [20] V. I. Zagrebaev, Prog. Theor. Phys. Suppl. No. **154**, 122 (2004).
- [21] Y. Aritomo, Phys. Rev. C **75**, 024602 (2007).
- [22] http://www.phy.anl.gov/ria/ria_yields/reaccelerated.html
- [23] J. Nolen, private communication.
- [24] Y. T. Oganessian *et al.*, Phys. Rev. C **74**, 044602 (2006).
- [25] Isotope Science Facility at Michigan State University, MSUCL-1345, November 2006 (unpublished).
- [26] R. Bass, Nucl. Phys. **A231**, 45 (1974).
- [27] K. Siwek-Wilczynska and J. Wilczynski, Phys. Rev. C **64**, 024611 (2001).
- [28] K. Siwek-Wilczynska, I. Skwira, and J. Wilczynski, Acta Phys. Pol. **34**, 1867 (2003).
- [29] W. J. Swiatecki, K. Siwek-Wilczynska and J. Wilczynski, Phys. Rev. C **71**, 014602 (2005).
- [30] P. Moller, J. R. Nix, W. D. Myers, and W. J. Swiatecki, At. Data Nucl. Data Tables **59**, 185 (1995).
- [31] P. Armbruster, Annu. Rev. Nucl. Part. Sci. **35**, 135 (1985).
- [32] J. D. Jackson, Can. J. Phys. **34**, 767 (1956).
- [33] R. Vandenbosch and J. R. Huizenga, *Nuclear Fission* (Academic, New York, 1973), p. 323.
- [34] W. D. Myers and W. J. Swiatecki, Phys. Rev. C **60**, 014606 (1999).
- [35] A. Ignatyuk, *et al.*, Sov. J. Nucl. Phys. **21**, 612 (1975).
- [36] C. Düllmann and K. E. Gregorich, private communication.
- [37] W. Neubert, Nucl. Data Tables **11**, 531 (1973).
- [38] See EPAPS Document No. E-PRVCAN-76-029708 for plots of nuclidic production rates. For more information on EPAPS, see <http://www.aip.org/pubservs/epaps.html>.
- [39] A. Sobieczewski and A. Parkhomenko, Phys. At. Nucl. **69**, 1155 (2006).
- [40] G. Audi, A. H. Wapstra, and C. Thibault, Nucl. Phys. **A729**, 337 (2003).
- [41] D. S. Brenner, N. V. Zamfir, and R. F. Casten, Phys. Rev. C **50**, 490 (1994); **55**, 974 (1997).
- [42] A. M. Vinodkumar, W. Loveland, P. H. Sprunger, D. Peterson, J. F. Liang, D. Shapira, R. L. Varner, C. J. Gross, and J. J. Kolata, Phys. Rev. C **74**, 064612 (2006).